VST project: technical overview

Dario Mancini, Giorgio Sedmak, Massimo Brescia, Fausto Cortecchia, D. Fierro, et al.

Dario Mancini, Giorgio Sedmak, Massimo Brescia, Fausto Cortecchia, D. Fierro, Valentina Fiume Garelli, Gabriella Marra, Francesco Perrotta, F. Rovedi, Pietro Schipani, "VST project: technical overview," Proc. SPIE 4004, Telescope Structures, Enclosures, Controls, Assembly/Integration/Validation, and Commissioning, (2 August 2000); doi: 10.1117/12.393895

SPIE.

Event: Astronomical Telescopes and Instrumentation, 2000, Munich, Germany

The VST Project: Technical Overview

D. Mancini[1], G. Sedmak[2], M. Brescia[1], F. Cortecchia[1], D. Fierro[1],
V. Fiume Garelli[1], G. Marra[1], F. Perrotta[1], F. Rovedi[1], P. Schipani[1]

[1]Osservatorio Astronomico di Capodimonte (OAC)
Technology Working Group (TWG)
Via Moiariello 16, I-80131 Napoli (Italy)

[2]Università di Trieste
Piazzale Europa 1, 34127 Trieste (Italy)

ABSTRACT

The VST (Very Large Telescope Survey Telescope) is an 2.6 m class Alt-Az telescope which will be installed in the European Southern Observatory (ESO) Paranal site, Chile. It has been designed by the Technology Working Group (TWG) of the Astronomical Observatory of Capodimonte (OAC), Italy. The VST is an 1°x1° wide-field imaging facility planned to supply databases for the ESO VLT science and carry out stand-alone observations in the UV to I spectral range starting in the year 2001. All the solutions adopted in the VST design comply to the ESO VLT standards. This paper reports a technical overview of the telescope design.

Keywords: telescopes, active optics, astronomical surveys

1. INTRODUCTION

The VST program is a co-operation between OAC and ESO regulated by a Memorandum of Understanding approved by the ESO Council on June 1998. The VST is a survey telescope, which will be located in the same area as the ESO VLT. When used in combination with the VLT units it will have the potential of allowing astronomers to reach the frontier in ground-based optical astronomy at truly high spatial resolution. For this reason the VST design has been carefully done in order to produce sharp and stable images. In addition, careful attention, paid to the telescope thermal control in combination with active optics, allow improving the angular image size beyond the performance of even larger but older telescopes. The VST design strategy has been defined in order to guarantee the optimization of the whole system and its technological sub-components. The strategy is based on the optimization of the integration of all subsystems into the system itself. Due to the complexity of the telescope design this strategy has been taken into account along the whole design work. In order to maintain the full control of the design activities the budget, times, performance and risks have been constantly monitored. The activities have been scheduled in detail in order to optimize the integration and test phases planned in Europe. This was done in order to reduce the general risk for all activities to be done at the final destination in Paranal site as well as for increasing the general reliability of the entire operation. A technical overview of the VST design is presented in the following sections.

2. IMAGE QUALITY BUDGET

The telescope error budget is used in order to establish system and subsystems requirements so as to comply with the required final optical quality. These requirements will define the complexity of the telescope itself. The error budget is a good criterion to design the whole telescope as an integrated system. Within a telescope the error sources contributing to the error budget can generally be addressed by reference to their effect on the image quality. The image quality budget includes all error sources, which affect the phase at the telescope focus after active optics correction. In fact the optical quality includes the effects of all residual errors after that active corrections have been applied. Since the images observed with ground-based telescopes are dominated by atmospheric seeing, it is more convenient and practical to evaluate the telescope error budget by means of the Central Intensity Ratio (CIR). This solution is better than the classical long-exposure optical

In *Telescope Structures, Enclosures, Controls, Assembly/Integration/Validation, and Commissioning*, Thomas A. Sebring, Torben Andersen, Editors,
Proceedings of SPIE Vol. 4004 (2000) • 0277-786X/00/$15.00

functions, such as the modulation transfer function (MTF), the point spread function (PSF) and the encircled energy (EE) [1]. The CIR is an intensity-based figure defined as the ratio of the central intensity given by the actual telescope to the central intensity given by an equivalent perfect telescope. It can be shown that the CIR is primarily dependent on the rms slope error σ of the wavefront generated by the telescope. If the rms slope error of the wavefront is known the CIR can be estimated on the basis of the following approximated formulas:

- for any wavefront error except random tilt

$$CIR = 1 - 2.89\left(\frac{\sigma}{\theta_0}\right)^2$$

- for random tilt (image motion)

$$CIR = 1 - 5.98\left(\frac{\sigma}{\theta_0}\right)^2,$$

where θ_0 is the full width at half maximum of the atmospheric seeing angle. Assuming that the individual errors are not correlated, the CIR variation associated with the combination of N individual error sources is simply the linear sum of individual CIR_i variations, i.e.:

$$1 - CIR = \sum_{i=1}^{N}(1 - CIR_i)$$

This expression is formally equivalent to the rule of the sum of the squares of individual rms slope errors. The total CIR decreases if the sum of individual errors decreases. The VST budget breakdown is composed essentially of the following errors:

- Telescope optical design. Due its large field of view the VST optical design introduces degradation with respect to the on-axis quality of a classical telescope.
- Surface errors. These include any deviation of the actual optical surface from the theoretical one. Under this label there are also included errors due to optics manufacturing, telescope and optics thermal deformations and mirrors supports system type and geometry. Optics positioning errors are not included under this label.
- Alignment errors. These include all optics positioning errors of the nominal optical surfaces (quasi-DC errors) and the errors due to the sensors of the control system (guiding and sensing system). Also included here are the errors produced by mechanical manufacturing, mounting, flexures, thermal expansions and thermal gradients. The scientific camera has been taken into account for its influence over the telescope behavior (mechanical and control).
- Control error cover the error budget for active optics and guiding and sensing system. The guiding accuracy takes into account all error sources that generate an image motion during the exposure time.
- The environmental effects on the final image are estimated with respect to the dome seeing and the wind buffeting. For dome seeing it is meant all the turbulence occurring close to the telescope that is not part of the free atmospheric turbulence. The dome seeing and the wind buffeting are indirectly correlated. Therefore the associated error budgets are correlated to avoid over-constraining of the telescope design. All image motion error sources that cannot be taken into account within the image motion error must be taken into account under within the wind buffeting error.

The overall error budgets of the available VST optical configurations (see section 3) are summarized in Tab. 1 at zenith and at 50° zenithal angle. The worst cases take into account the effects of the wind on optics, while the best cases do not take them into account.

VST Optical Configuration	Expected CIR Worst/Best case
Two-lens (z=0°)	0.4727 / 0.5131
ADC & one-lens (z=0°)	0.3551 / 0.3961
ADC & one-lens (z=50°)	0.3466 / 0.3876

Tab. 1 - VST expected performances in terms of CIR

3. OPTICS

The VST is a 2.61m Alt-Az f/5.5 modified Ritchey-Chretien telescope. It is optimized in order to correct a very large field of view (FOV) for a high spatial resolution. The corrected FOV of 1°x1° will be matched with a 16k x 16k CCD mosaic camera to be provided by the European Omegacam Consortium under a Memorandum of Understanding signed with ESO in January 2000. The VST is provided with two different correctors made with refracting and dispersing elements. In order to cover the wide field of view with a high image quality the telescope design is optimised together with the correctors and camera optics including the CCD mosaic cryostat window. The first corrector is made of two lenses and operates in the range from 320 nm to 1014 nm with observing angles relatively close to zenith. The second corrector is made of a rotating Atmospheric Dispersion Corrector (ADC) and an additional lens and operates in the range from 365 nm 1014 nm. This last corrector operates from zenith down to 70° zenith angle. The ADC glasses have been chosen in order to minimize the pupil motion with respect to the ADC rotation. The solutions found for correctors show a nominal optical quality, which is very close to the goal. The layout of the ADC and one-lens corrector and of the two-lens corrector is shown in Fig. 1 and respectively in Fig 2. The top-level scientific requirements for the optical image quality and performance are summarised in Tab. 2. The image quality has been evaluated by means of the polychromatic diffraction encircled energy diameter at 80% level and also by means of CIR [3] in order to take into account the atmospheric seeing.

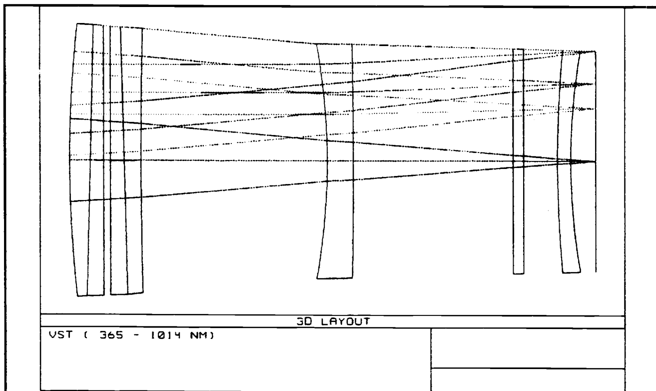

Fig. 1 - Zoom of the optical layout of the VST corrector with the ADC and one lens (B - I bands)

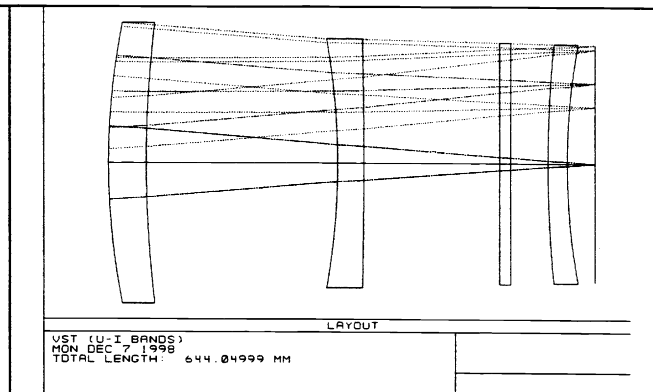

Fig. 2 - Zoom of the optical layout of the VST two-lens corrector (U ÷ I bands)

Telescope aperture		2610 mm
Image Scale		0.21 arcsec/pixel
Pixel reference size		15 μm
Un-vignetted field of view		1.47° diagonal
Image quality (EE)	Required	80% within 2 × 2 pixels
	Goal	80% within 1 × 1 pixel
	As designed two – lens	80% in 1.33 pixel at z = 0° (worst case, edge of the field)
	As designed ADC and one-lens	80 % in 1.53 pixel at z = 0° 80 % in 2 pixel at z =50° 80 % in 2.8 pixel at z =70°
Image quality (CIR)	Requirements:	none
	As designed Two – lens	0.8157
	As designed ADC and one-lens	0.698 at z=0° 0.690 at z=50° 0.675 at z=70°
Maximum distortion		≤ 0.3% required, ≤ 0.01% goal, 0.013 % (as designed, worst-case)

Tab. 2 - Main requirements and as designed performance of the VST optical image quality

The ghost analysis shows that no bright focused ghosts will appear on the CCD and a very low level of sky concentration is created (0.0004). The manufacturing errors, which cannot be compensated by active optics control, produce higher order errors. Based on actual optical fabrication quality standards for mirrors a high frequency RMS error of about 30 nm is expected. The thermal analysis has been done following the results of ESO studies of the daily/nightly temperature variations at Paranal site. As concerns the hourly temperature variations a mean value of ± 1.7 degrees/hour can be assumed as a typical upper value. A focus change analysis has been performed for both corrector configurations. The nightly analysis has been done for an excursion of ± 4.2 °C. The maximum nightly focus change is well within the telescope focus depth of 160 μm. When the system is refocused, the imaging performance is maintained with a longitudinal displacement of the secondary mirror of a just a few microns. When all telescope optics are properly aligned only residual aberrations are present in the whole field. Optical aberrations are introduced by thermal deformation of the mechanics, misalignments of the secondary mirror, and optical distortions of the primary mirror due to its sensibility to the structural deformations of the cell. An active control system is used in order to guarantee the correct alignment.

4. ACTIVE OPTICS

The aberrations corrected by the VST active optics control system are essentially the coma, defocus (secondary mirror re-alignment) and the spherical, astigmatism, quad-astigmatism and tri-coma (primary mirror sag deformation) aberrations. The VST band-pass for active optics ranges from DC to 1/30 Hz. The limit of 1/30 Hz corresponds to an integration time of 30 seconds, which is sufficient to integrate out the external seeing and produce a round image corresponding to the integrated external seeing quality. The Adapter/Rotator of the VST foresees a sensing and guiding arm that provides the telescope guiding and the on-line wavefront analysis if required. The wavefront analysis system is based on a Shack-Hartmann sensor and is sensitive enough to work on guide stars of magnitude +14 for integration times of the order of 30 seconds: The size of the VST pupil sampling sub-apertures is of the order of 250 mm. The number of the Shack-Hartmann spots across the telescope pupil is equivalent to 10. The lenslet array used shows a f/45 focal number and a lenslet diameter Dl ≈ 0.5 mm. It fulfils all requirements for the optimum choice of a Shack-Hartmann analyzer [4]. The guiding and sensing arm is mounted on a rotating support coaxial with the rotator and its optics is mounted on a radial rail. These two devices implement a polar system, which allows reaching the center of telescope field during the off-line calibration phases. The polynomial base used to fit the wavefront is composed by the elastic mode of the primary mirror itself. In this way the energy required to deform the primary mirror is minimized. The VST primary mirror is supported by means of axial and lateral pads. The axial pads are distributed on four rings, which include respectively 12, 18, 24 and 30 pads. The axial pad distribution has been analyzed also by means of Finite Elements Analysis (FEA) as described in the next section. The 24 lateral pads are designed to be VLT-like. The forces are applied at the center of the rim and the force vector lies in the neutral plane at the outer edge. The calibration forces required to generate a given elastic mode with a wavefront rms error of 1000 nm are shown in Tab. 3. These data have been verified by FEA calculations. The table lists the maximum forces on each ring. The forces for each support can be obtained by multiplying the maximum forces with the cos (n*phi_i, j), where phi_i, j is the j-th support on the ring i and n is the order of rotational symmetry. Also the secondary mirror support performs the required actions in a smooth way with high positioning resolution and accuracy. The secondary mirror movement accuracy adds to the error budget 0.0167 arcsec for the defocus correction, 0.0105 arcsec for the coma correction and 0.015 arcsec for the image displacement on the focal plane not corrected by means of any tip-tilt system. These parameters involve the possibility to perform mirrors alignments and focus corrections without the need to temporarily stop the observations. These conditions can be achieved making use of a special customized device based on a two-stage system for positioning the secondary mirror. The first stage is a standard hexapod (HEX#1), while the second stage is a very high resolution X, Y, tilt and piston piezoelectric system (HEX#2). The HEX#1 system moves the secondary mirror during the pointing phase and between the acquisition of two frames. It does not operate during the acquisition of a frame. The HEX#2 system moves the secondary mirror during the science image acquisition with a range smaller than HEX#1 but with a very high resolution and accuracy. The high stiffness of HEX#1 guarantees the absolute positioning of the secondary mirror during tracking. The total ranges for both HEX#1 and HEX#2 systems have been computed taking into account the gravitational and thermal deformations and the range of compensation for the optical tolerances, (Tab. 4 and Tab. 5).

Rotational symmetry	Order of mode	Ring 1 (N)	Ring 2 (N)	Ring 3 (N)	Ring 4 (N)
0	2 (sph)	682.548	-391.934	-442.203	345.904
2	1 (ast)	1.817	5.176	8.455	11.193
3	1	4.593	22.572	45.366	70.151
4	1	4.561	52.395	127.316	225.736

Tab. 3 - Calibration forces for the axial pads of the primary mirror to generate an elastic mode with an rms error of 1000 nm

5. FEA ANALYSIS

As underlined above the use of Finite Element Analysis calculations in the VST design strategy guarantees the optimization of the whole system in terms of mechanical design and optical interfacing. Some of the most important results from FEA work are described in the following.

1. Primary Mirror FEA

The analytical treatment of the problem of the computation of the deformation of a thin mirror due to the gravity is based on the assumption that the mirror is approximated by means of a curved surface supported by three or four continuos rings centered on the mirror center. The optimization is based on the minimization of σ_w (rms value of the wavefront error). The parameters are the radii of the rings and the fraction of the total load on each ring. The numbers of supports on each ring are chosen considering the number of supports, that should be multiples of three, and the azimuthal distance between the supports on one ring, that should approximately be the same of the distance between the rings in radial direction. The final choice for the VST is a four ring distribution. The configuration reached over the full aperture is shown in Tab. 6.

Parameters	HEX#1 Theoretical Characteristics	Target Values
Travel X [mm]	±10	± 0.4
Travel Y [mm]	±10	-
Travel Z [mm]	±20	± 3.5
Travel θx/θy [o]	±3.0	± 0.05
Resolution X/Y [μm]	2	7
Resolution Z [μm]	1	2.29
Repeatability X/Y [μm]	±4	-
Repeatability Z [μm]	±2	-
Repeatability θx/θy [arcsec]	±2	-

Tab. 4 - Parameters of the HEX#1 system for M2 positioning

Parameters	HEX#2 Theoretical Characteristics	Target Values
Travel X /Y	180μm	152 μm
Travel Z	180μm	119 μm
Travel θx/θy	0.0206°, (74.25 arcsec 180μm**)	0.00307°, (11arcsec-27μm**)
Resolution X/Y	1.2 nm	0.5 μm
Resolution Z	1.2 nm	0.5 μm
Repeatability X/Y	±2.4 nm	-
Repeatability Z	±2.4 nm	-
Repeatability θx/θy	± 0.001 arcsec	-

(**) The computation of the linear range has been done taking into account an arm equals to 500 mm

Tab. 5 - Parameters of the HEX#2 system for M2 positioning

Ring	r_i(ring radii, mm)	ρ_i, (normalized ring radii)	f_i, (load fraction on each ring)	Pad Number	f_i/ρ_i
1	427.55	0.321709	0.134410	12	0.4178
2	704.11	0.529804	0.228627	18	0.4315
3	971.53	0.73102	0.304733	24	0.4169
4	1228.82	0.924623	0.332230	30	0.3593

Tab. 6 - Results of the optimization for a four rings configuration

In order to verify the accuracy of the analytical procedure a comparison has been done with the finite element analysis in terms of σ_w (rms value of the wavefront error). The FEA analysis confirms the analytical results. An equivalent procedure has been followed to evaluate the forces to be applied on the 24 lateral pads of the primary mirror when it is not in the horizontal position. The plane passing through the lateral pad is not placed at the level of the center of gravity. A VLT-like support has been used. The force is applied at the center of the rim that identifies the pads and the force vector lies in the neutral plane at the outer edge. An FEA Analysis has been performed in order to evaluate the optical quality degradation due to the gravity load when the mirror is vertical. In Fig. 3 the results of the FEA are shown in terms of the primary mirror surface sag.

Fig. 3 - Primary mirror deformations along Z axes for 90 degrees load case

6. MECHANICAL DESIGN

The telescope mechanical design follows the optical configurations to be provided and the positioning accuracy required for each optical element. After obtaining the best possible positioning accuracy through the structural analysis for all the configurations the design of the telescope mount has been preliminarily balanced. The mount has been studied for its vibration properties, which set limits on the drive system responses to tracking and pointing errors. Mount vibration and stiffness properties also drive how the telescope will respond to wind buffeting. The power spectral density of the wind disturbance torque, as described by the Von Karman spectrum, shows that the performance is mainly influenced by the spectral components up to 0.1-1 Hz. At higher frequencies the wind disturbance decreases and can be considered negligible. Large masses in the structure are avoided because they limit the structure frequencies and create thermal reservoirs that can spoil local seeing conditions. Not surprisingly, the mechanical design is an iterative process. For this reason the following items have been taken into consideration:

- Telescope size. One of the main goals is to make the telescope compact enough in order to reduce the size and cost of the telescope itself and of the required surrounding enclosure. The optics design is compact and allows reaching the mentioned goal. The mechanical design is optimized around the optical design.

- Structural stiffness. It has been maximized but not at the expense of an excessive weight. Misalignments of the optics due to non-elastic gravitational flexures have been avoided by means of an accurate analysis of the mechanical subsystem design and an accurate evaluation of the technical characteristics of the components. Misalignments of the optics due to the elastic gravitational flexures have been carefully analyzed, predicted by means of Finite Element Analysis and included in the global error budget computation. The mechanical design has been optimized on the base of repetitive structural performance analyses used to feedback the mechanical design.

- Weight/Mass/Stiffness and Thermal Properties. The design of the telescope has been done also with the aim to optimize Mass/Stiffness ratio and to avoid large thermal inertia. This task has been done with the aim to have the overall time constant smaller than one hour anywhere in the structure. The overall spring constant for the assembled telescope structure is large enough to maintain the lowest structural resonance above the limits imposed by the general telescope performance requirements. This limit has been pointed out by the Control System Performance analysis and by the need to meet the General Telescope Performance Error Budget. The higher is the lowest structural resonance (locked rotor frequency) the higher can be the bandwidth of the control loop. The study of the dependence of the wind disturbance rejection on the control loop bandwidth has given the results shown in Tab. 7 and in Fig. 4. The expected bandwidth of the control loop is fixed to be 3 Hz, corresponding to a max rms displacement due to wind of about 0.14 arcsec. Lower bandwidth values would introduce higher errors.

Bandwidth [Hz]	RMS error [arcsec] Worst case (α_2=0.98)	RMS Error [arcsec] Worst Most Favorable Case (α_3=0.63)
2	0.18	0.04
3	0.14	0.03
4	0.12	0.02
5	0.11	0.02

Tab. 7 - Axis rotation due to the wind for various control loop bandwidths

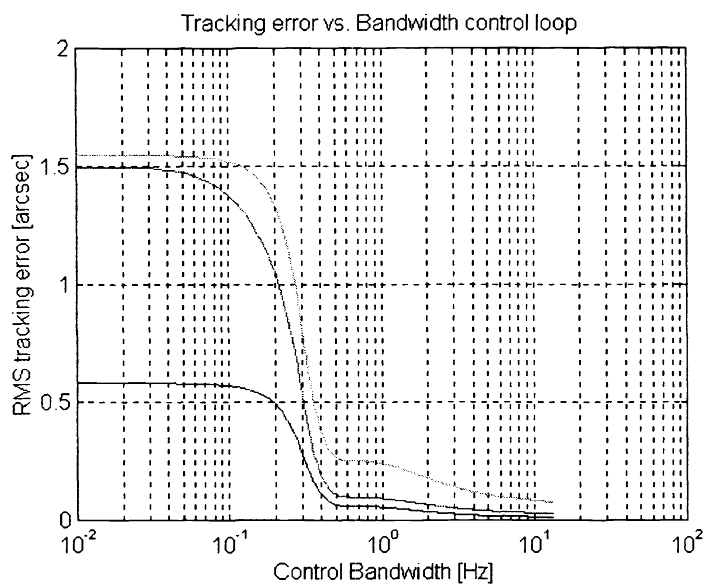

Fig. 4 - Tracking error vs. ctrl loop bandwidth (wind speed reduction due to the enclosure R: α_1=1, G: α_2=0.98, B: α_3=0.63)

- Thermal control. Temperature differences between the telescope and the surrounding air is kept in the range of +/- 1 °C to avoid thermal turbulence in the light path. Thermal gradients in the structure cause tip-tilt and defocus of the secondary mirror, which is controlled and actively adjusted before and during any observation. In addition, all the subsystems are cooled and actively controlled in order to maintain the surface temperatures in the range +/-1°C with respect to the ambient.

- Maintenance and accessibility. All subsystems are designed in order to allow easy maintenance and full accessibility.

- Earthquake protection. The telescope is designed to withstand the predicted accelerations without damage. The primary will be protected for radial and axial solicitation.

- Wind effects. In normal operation air will intentionally be allowed to flow around and through the telescope in order to minimize the temperature gradients and their effects on the local seeing. The telescope structure has been designed in order to permit a smooth airflow and to maintain a stiff optical alignment for wind velocities up to 18 m/sec. The wind disturbance effects on tracking performance have been evaluated to be about 0.15-0.2 arcsec rms in the worst possible conditions (frontal wind on altitude axis without any wind speed reduction inside the enclosure). In more favorable wind direction conditions and taking into account a wind speed reduction factor up to 0.63 inside the enclosure, the rms tracking error induced by the wind has been evaluated to decrease down to 0.03-0.05 arcsec.

- Driving accuracy and smoothness. Errors affecting a smooth rotation shall be restricted to amplitudes, measured in rms image motion in any focal plane, of less than 0.02 arcsec. To satisfy these requirements an Hydrostatic Bearing System is used to obtain excellent smoothness and low friction.

2. Telescope Structure FEA

As underlined above the mechanical design is an iterative process and for this reason it has been performed taking into account the feedback from the finite element analysis of its structure. The main actions performed with FEA on the VST mechanics were:

- Compute the axes first resonance frequencies
- Test the effects of the wind and gravity loads on the relative tilt decentering and defocusing of the mirrors
- Compute the actual stiffness between the parts of the telescope to be used in the telescope model for the control system
- Verify that no elements in the structure are stressed over their proper limits

The gravitational load analysis has been considered with the telescope at elevation 0° and 90°. The wind has been considered both statically and dynamically with the telescope in different positions. The presence of the pillar has been simulated in the FEA in order to optimize the whole assembly telescope/pillar in terms of dynamical performance and in order to verify that the total amount and spectrum of the vibrations comply with the VLTI activities.

The earthquake response spectrum has been also considered at the level of the soil bottom layer in order to verify the reliability of the complete structure of the telescope in case of seismologic events. The calculated acceleration field has been applied to the three-dimensional model of the primary mirror, which is considered constrained by its axial and radial pads, in order to verify that the stresses induced do not exceed the maximum allowable value for mirror material (SITAL).

7. TELESCOPE CONTROL SYSTEM

1. Introduction

The design of the VST telescope control system is based on the main concepts used by ESO for the VLT design. This choice simplifies the VST maintenance programs and ensures a full and fast integration of the telescope in the VLT environment at Paranal. In addition, the optimization of the control of the main telescope subsystems has been reached whenever feasible by preferring software solutions instead of a full hardware strategy. The basic advantages given by this approach are a high flexibility during the development, the maintenance and the system upgrading.

2. Control hardware

The VST control system consists of two workstations, used to manage the Telescope Control Software (TCS) and the Guide/Acquisition system, plus several distributed Local Control Units (LCUs) as shown in Fig. 7. The LCUs implement the complete control of all the sub-systems by means of digital, analog or serial connections. Some subsystems, such as active control of the primary and secondary mirror and the hydrostatic bearing support for the azimuth rotation, will be driven by dedicated controllers under the supervision of the main LCUs, which will also maintain the full diagnostics of any function or status. All the telescope control functions are distributed in the control cabinets as shown in Fig. 8. Any axis motor torque command is provided by the LCUs to the motor power amplifiers by means of a 16-bit DAC board. The speed loop is closed by means of four tachometers coupled to the motor axes through a high performance 16 bit A/D converter, used to get over-sampled tachometer readouts. The position loop is closed by means of the Heidenhain ERO7001 encoders and associated electronics, successfully used in past realizations. The quantization effect due to the position servo loop is reasonably rejected due to the high frequency of the servo loop, which is set to 500Hz.

8. DRIVE SYSTEM

Each axis incorporates four brushless motors controlled in pairs. A torque preload is applied between each motor couple in order to compensate for the backlash in the telescope pinion/gear coupling.. The preload torque function is obtained by means of an adaptive software algorithm, which is included in the control system. The algorithm regulates each motor preload torque value according to the instantaneous axis acceleration and/or the instantaneous total torque required. The drive system design is matched to the mechanical design in order to comply with the motion smoothness requirements. The drive system accuracy is able to satisfy the pointing requirements. The range accessible in zenith distance shall be from 1 degree, with a goal of 0.5 degree, up to 70 degrees. With a pointing model based on the measurement of no more than 30 stars the absolute pointing shall be better than 5 arcsec rms for zenith distances up to 60 degrees. Relative offsets up to 3 degrees shall be accurate to within 0.5 arcsec. The smoothness of the motion is ensured and undesired frictions in the motion are reduced to the lowest possible limit in order to satisfy the tracking requirements up to zenith distances of 60 degrees and wind speeds of 18m/s with a dynamical component of 30%. The free tracking performance of the telescope shall be better than 0.2 arcsec rms. With closed-loop auto guiding, the rms tracking deviation will be smaller than 0.1 arcsec.

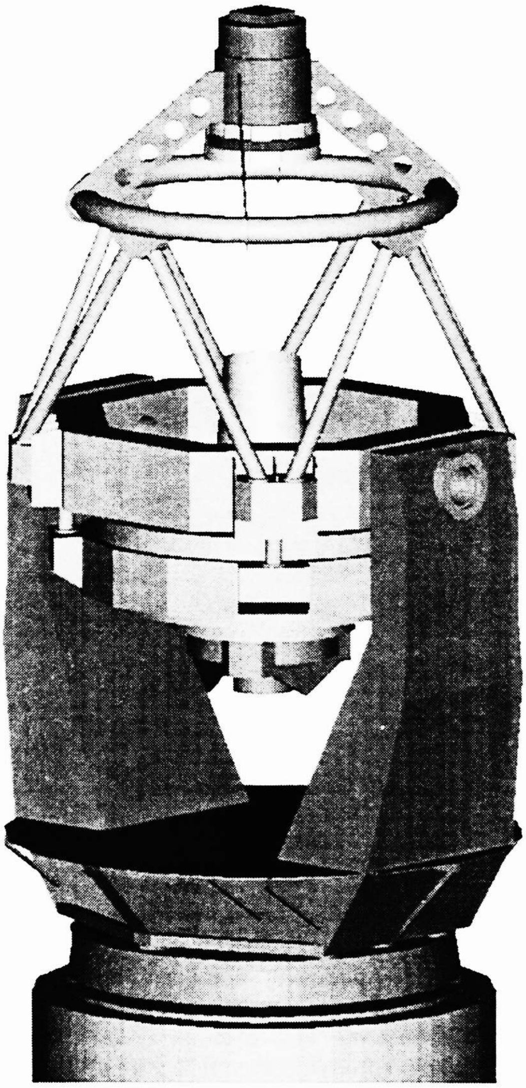

Fig. 5 - A render view of the VST

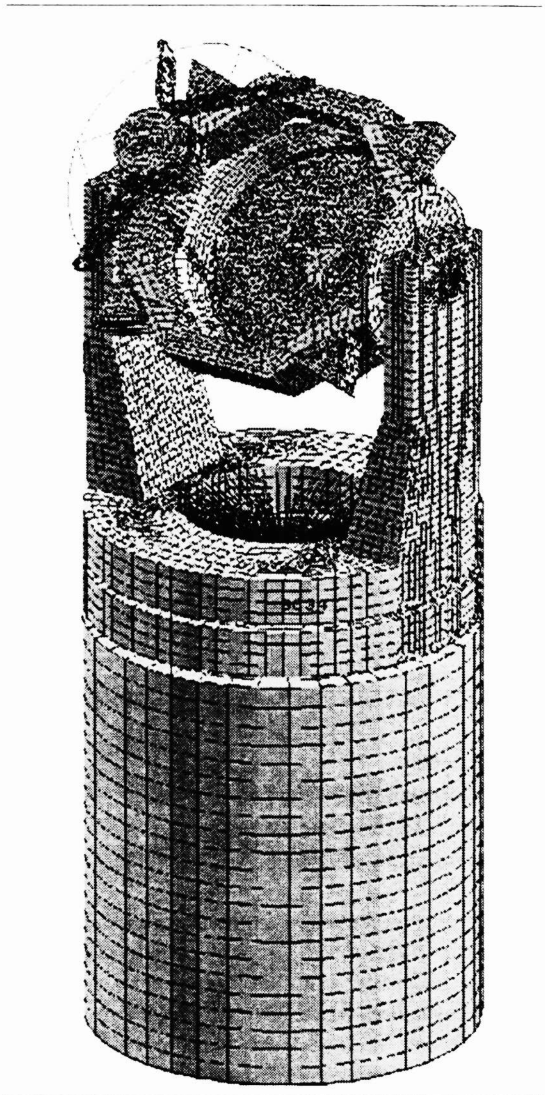

Fig. 6 - Telescope and pillar F.E. model.

9. CONTROL SOFTWARE

The VST Telescope Control Software (TCS) is the software package responsible to implement:

- Control and monitoring of the telescope

- Interfacing to users and other VST software packages
- Interfacing to star catalogues

This means that the TCS takes care of the control of the main axes (altitude and azimuth), the mirrors, the Cassegrain instrument adapter/rotator, the Technical Charge Coupled Devices (TCCDs) for auto guiding and active optics control, the Atmospheric Dispersion Correction (ADC) system, the enclosure, and other auxiliary equipment. The TCS makes extensive use of the VLT Common Software, which provides common services, utilities and communication tools. The VLT TCS is a general software package that will be re-used on the VST to a large extent. The functional scheme of the TCS foreseen for the VST telescope is shown in Fig. 9.

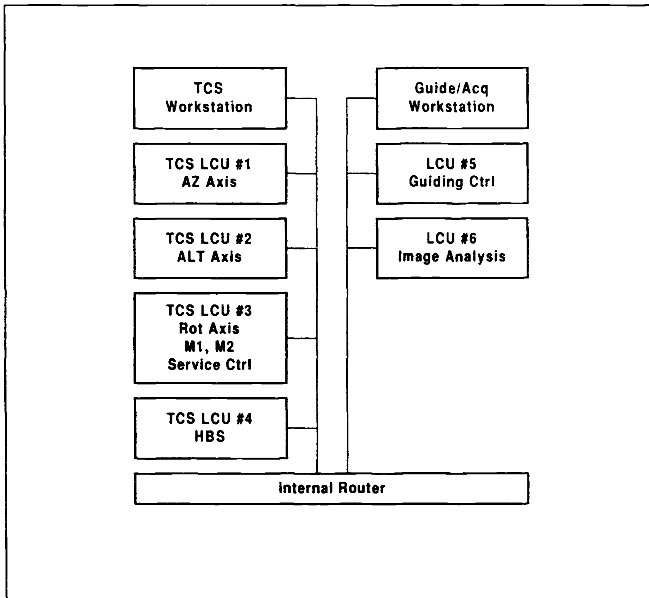

Fig. 7 - Telescope Control Architecture

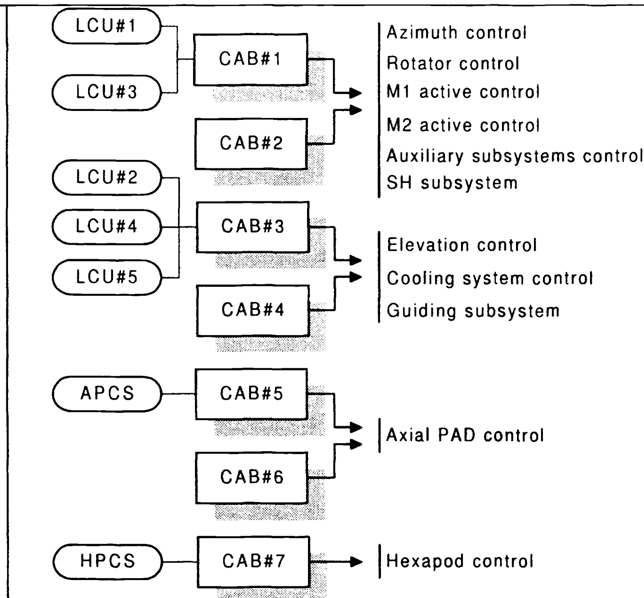

Fig. 8 - Control System Architecture

The VST TCS software can be grouped in four main categories:

- User interface
- Coordinating software
- Subsystem application software
- Special interface software

The coordinating software is hierarchically below the user interface and above the subsystem software, in the sense that it performs actions of combined and coordinating nature. It may use one or more subsystems to execute its actions. The coordinating software runs on the system workstation (WS). The subsystem application software implements all the functions that need to be performed locally in an LCU without any knowledge about other system components. The special interface software is based on a group of libraries with the task to access via the TCS external systems like the star catalogues. A particular role is performed in the VST TCS by the coordinating software, which provides a public interface for external applications requiring services to the TCS through functional software modules basically composed by specialized processes running concurrently on the TCS WS. The main modules included in the coordinating software manage the presetting, the tracking, the auto guiding, the enclosure control and the active optics control. Each module is provided with a Command Definition Table (CDT) which is normally used for all inter-module communications and is also used by the TCS user interface panels. In the TCS general module architecture all the modules are implemented through one or more independent processes. If a module is made up of more than one process only one of them is the "control" process which provides the public interface, receives commands from other modules and sends back the corresponding replies. In order to respect these requirements every process is designed in an event-driven way and the implementation is based on the event-handler design. The TCS package is composed by several modules associated to the telescope subsystems to be handled by the TCS. Each module is organized in processes and functions dedicated to the LCU and/or WS resident applications. The applications use specific commands to perform all the actions foreseen for the control and management of the associated subsystem. For the main axes, azimuth and altitude, the software will run on dedicated LCUs and execute commands from the TCS higher level modules. The software running on the LCUs is a low-level part of the TCS that is interfaced only with the local axis to be controlled. All axes are considered independent. The correlation of the motions of the axes, which occur when the telescope is tracking an object, is achieved through a very accurate time synchronization of the relevant LCUs.

The software module for the active optics control will run on the VST WS and will perform the following main actions:

- Primary mirror (M1) active optics control software workflow. Comparison between the information in terms of the expected actuators positions coming from the Shack Hartmann wavefront sensor analysis and the current actuators positions which depend on the actual temperature and the telescope elevation. This information allows determining the corrections to be applied for obtaining the wanted actuators positions.
- Secondary mirror (M2) active optics control software workflow. Comparison between the information in terms of the expected hexapod legs positions coming from the Shack Hartmann wavefront sensor analysis and the current hexapod actual legs positions which depend on the telescope elevation. This information allows to determine the corrections to be applied for obtaining the wanted hexapod legs positions

The corrections for the field aberrations and the field orientation are also calculated on the VST WS. The information on the forces to be applied to M1 and the repositioning to be done on M2 are sent to the M1 and M2 LCUs, which perform the analysis of the Shack Hartmann image and determine the aberrations to be corrected.

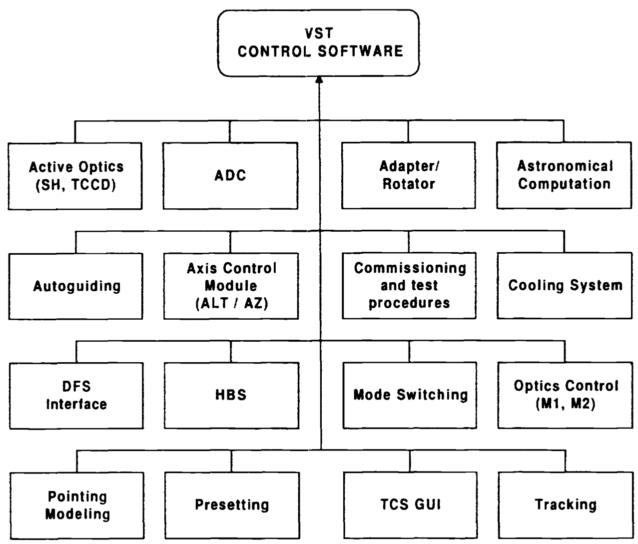

Fig. 9 – VST Control Software Module Layout

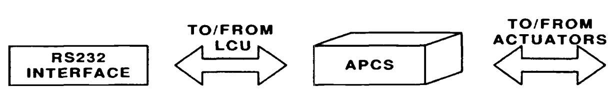

Fig. 10 – M1 Active Optics Control Layout

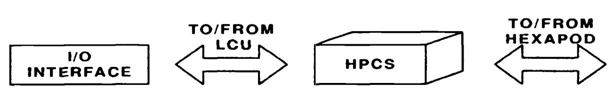

Fig. 11 – M2 Active Optics Control Layout

The M1 active optics control system is based on the control of the mirror support plates through the Axial Pad Control System (APCS) that is responsible for the active control of the VST primary mirror. A TCS LCU will communicate with the APCS at higher level through a series of macro-commands. It will receive the diagnostics on the single APCS sub-units via a standard RS232 serial link. The APCS will take care of the low-level execution of the relevant macro-commands in an asynchronous mode. The APCS will control 81 astatic levers positioned under the primary mirror and read the load cells positioned under three fixed points. A schematic layout of the APCS system is shown in Fig. 10. The M2 active optics control is based on a dedicated electro-mechanical Hexapod Positioning Control System (HPCS) that interfaces the TCS with the hexapod system. This last system consists of a pair of movable platforms positioned by means of piezoelectric and linear actuators as shown in the layout of Fig. 11. The HPCS is based on a multi-processor architecture, which includes a fast Digital Signal Processor (DSP) motion control chip set. The DSP provides the generation of the trajectory data and the closed loop digital servo control based on the position information supplied by incremental encoders. A host processor is used for communications and the command handling. The operating software (firmware) receives the motion commands via standard I/O communications from the host LCU. It will be equipped by a series of very flexible and powerful macro-commands, which give the possibility to the TCS qualified operators to easily perform the required calibration procedures.

10. CONCLUSIONS

The high telescope design performance and the excellent Paranal site seeing make the VST competitive for the wide field imaging (WFI) in the southern hemisphere. The need for an ESO WFI facility such as the VST is very strong primarily as a complementary tool for the VLT and also as an independent survey tool and the support for stand-alone observational projects [7]. The ESO community needs a survey facility such as the VST in order to produce the sky databases, which are essential to achieve excellence in the science of the VLT era.

11. REFERENCES

1. Optical performance of large ground-based telescope, P. Dierickx, Journal of modern optics, 1992, vol.39, n°3, 569-588
2. VST Technical Proposal, Technology Working Group OAC Naples, 06.10.97
3. VST Preliminary Design Review, Technology Working Group OAC Naples, 15.01.99
4. VST Final Design Review Technology, Working Group OAC Naples, Issue 1.0, 06.12.99
5. Optimum choice of parameters and use of a Shack-Hartmann analyzer in telescope with active optics. L. Noethe , ESO Documentation
6. Reflecting Telescope II. Editor. Springer. R.N.Wilson
7. VST: VLT Survey Telescope, M.Arnaboldi, M.Capaccioli, D.Mancini, P.Rafanelli, R.Scaramella, G.Sedmak, G.Vettolani, The ESO Messenger N.93 (1998) 30-35